

TI-853

12 May 53

WADC TECHNICAL REPORT 52-226
PART 1

AD 8137 ✓

**INVESTIGATION OF AXIAL LOADING FATIGUE PROPERTIES
OF HEAT-RESISTANT ALLOY N-155**

**B. J. LAZAN
F. DE MONEY**

UNIVERSITY OF MINNESOTA

MARCH 1953

WRIGHT AIR DEVELOPMENT CENTER

20010501001

NOTICES

When Government drawings, specifications, or other data are used for any purpose other than in connection with a definitely related Government procurement operation, the United States Government thereby incurs no responsibility nor any obligation whatsoever; and the fact that the Government may have formulated, furnished, or in any way supplied the said drawings, specifications, or other data, is not to be regarded by implication or otherwise as in any manner licensing the holder or any other person or corporation, or conveying any rights or permission to manufacture, use, or sell any patented invention that may in any way be related thereto.

The information furnished herewith is made available for study upon the understanding that the Government's proprietary interests in and relating thereto shall not be impaired. It is desired that the Judge Advocate (WCJ), Wright Air Development Center, Wright-Patterson Air Force Base, Ohio, be promptly notified of any apparent conflict between the Government's proprietary interests and those of others.

WADC TECHNICAL REPORT 52-226
PART 1

**INVESTIGATION OF AXIAL LOADING FATIGUE PROPERTIES
OF HEAT-RESISTANT ALLOY N-155**

*B. J. Lazan
F. DeMoney*

University of Minnesota

March 1953

*Materials Laboratory
Contract No. AF 33(038)-18903
RDO No. 614-16*

Wright Air Development Center
Air Research and Development Command
United States Air Force
Wright-Patterson Air Force Base, Ohio

McGregor & Werner, Dayton, O.
250 May, 1953

FOREWORD

This report was prepared by the University of Minnesota under Contract No. AF 33(038)-18903. The contract was initiated under Research and Development Order No. 614-16, "Fatigue Properties of Structural Materials", and was administered under the direction of the Materials Laboratory, Directorate of Research, Wright Air Development Center, with Mr. W. J. Trapp acting as project engineer.

ABSTRACT

Dynamic creep and rupture data are presented on N-155 at room temperature and 1000° F., correlated to some extent with prior work. Temperature increases were observed in certain temperature and stress ranges immediately after the application of alternating stress to a test specimen. These are discussed in terms of the internal damping capacity of the material and the possibility of utilizing these observed temperature increases as a qualitative indication of damping is suggested. A vibration analysis of the Minnesota direct stress fatigue machine is presented and used to correlate calibration data procured by three independent methods.

PUBLICATION REVIEW

This report has been reviewed and is approved.

FOR THE COMMANDING GENERAL:

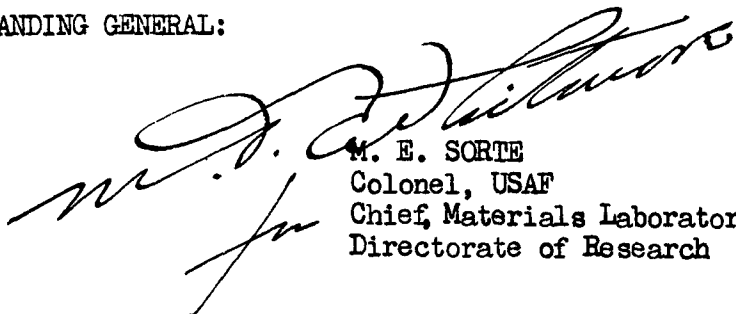

M. E. SORTE
Colonel, USAF
Chief, Materials Laboratory
Directorate of Research

TABLE OF CONTENTS

	Page
I. Introduction	1
II. Testing Machines and Their Calibration	1
III. Test Materials	7
IV. Test Specimens	7
V. Test Procedure, Test Data, and Discussion	7
VI. Summary and Conclusion	12
Bibliography	13

AXIAL FATIGUE PROPERTIES OF N-155 AT ROOM TEMPERATURE
AND 1000°F UNDER VARIOUS STRESS RATIOS

I. INTRODUCTION

This work represents a continuation of previous research conducted at Syracuse University (1) (2)* on Air Force Contract W33-038 AC15941. All the work reported in this part was conducted on low carbon N-155 at room temperature and 1000°F.

II. TESTING MACHINES AND THEIR CALIBRATION

2.1 Purpose and Scope

All data were procured in specially constructed direct stress machines developed for this work (1) (2). These machines have a capacity of 5000 lbs. mean force and \pm 5000 lbs. alternating force at 3600 rpm.

In view of certain irregularities which appeared during some of the earlier tests, a rather complete dynamic analysis and calibration program was undertaken on the fatigue machines used. The dynamic force analysis involved a theoretical and experimental study of the exciting force, inertia force, specimen elasticity, and phase angle relationships in the two mass and two spring systems which may be assumed to represent the fatigue machine.

Dynamic and static force and stress distributions calibrations were accomplished principally by measuring the strain in a specially prepared test specimen with SR-4 strain gages attached. This method was checked experimentally by direct measurements with a proving ring. Furthermore, the specimen force was theoretically determined by computing the centrifugal force exerted by the rotating eccentric and taking into account the approximate inertia forces involved and their phase relationships. These three methods of determining the specimen force are described in detail below.

*Numbers in parenthesis refer to references in the bibliography.

2.2 Strain-Gage Analysis

In the strain-gage method, three type C-1 SR-4 gages were cemented at positions 120° apart to a cylindrical alloy steel specimen having gage length of 2" and **diameter of 0.4"**. The temperature compensation gage was cemented circumferentially around the test length. To eliminate error due to the Poisson effect on the dummy gage, the dynamometer was calibrated in a static testing machine. Strain was measured by means of an Ellis bridge amplifier used in conjunction with a cathode ray oscilloscope. The stress in the specimen was computed from the average of the three strain gage readings so that the effects of bending would not affect the determination of the total force on the specimen. In the presence of bending in the specimen due to eccentric loading through the grips, the difference between readings of the three gages may be used to determine the bending stress. With the improved gripping devices (1), the average bending stress observed in test specimen was generally less than 4%.

2.3 Proving Ring Analysis

In a second independent experimental method of calibration, a Morehouse proving ring was employed. This ring, equipped with an electric contactor device in place of the usual vibrating reed, was inserted in place of the test specimen. The maximum load during a cycle was determined for various settings of the eccentric with the aid of a neon light to indicate contact.

2.4 Theoretical Analysis

As a theoretical check on the above experimental methods, the centrifugal force produced by the rotating eccentric and the relationship of this force to the force on the specimen were analyzed as outlined below.

The direct stress machines used in this work consist basically of the spring-mass system shown in Fig. 1. A heavy mass M_1 (frame and component parts) is mounted on springs K_1 , and a relatively small mass M (cage, preload springs, and component parts) is connected to the frame by another spring K (test specimen).

A sinusoidal force $F = F_0 \sin ft$, produced by the rotating eccentric, is applied to the small mass M which is constrained to move **only in the vertical direction**.

For this system it can be shown (3) that the amplitude of vibration A_1 of mass M_1 and amplitude A of mass M are given by the following equations:

$$A_1 = \frac{F K}{(M_1 f^2 - K_1 - K) (M f^2 - K) - K^2} \quad (a)$$

$$A = \frac{F (K_1 + K - M_1 f^2)}{(M_1 f^2 - K_1 - K) (M f^2 - K) - K^2} \quad (b)$$

where: f = angular frequency of the rotating eccentric in rad./sec.

If masses M and M_1 and K and K_1 are associated with the actual fatigue machine parts as indicated above, then the following constants may be substituted in equations (a) and (b).

$M_1 = 1370 \text{ lbs.} = 42.7 \text{ slugs} = \text{weight of frame and attached parts}$

$M = 55 \text{ lbs.} = 1.71 \text{ slugs} = \text{effective weight of cage and attached parts}$

$K_1 = 9000 \text{ lbs/in} = 108,000 \text{ lbs/ft} = \text{spring constant of springs which}$

isolate the frame from the floor to avoid vibration transmission

$K = 10^6 \text{ lbs/in} = 12 \times 10^6 \text{ lbs/ft} = \text{approximate spring constant of the test specimen.}$

Since K is much larger than K_1 , it can be shown that K_1 can be equated to zero without significantly affecting the behavior of the system. Doing this and defining $f_1^2 = K/M_1$ and $f_2^2 = K/M$, then equations (a) and (b) become:

$$A_1 = \frac{F/K}{(1 - f^2/f_1^2) (1 - f^2/f_2^2) - 1} \quad (c)$$

$$A = \frac{F/K (1 - f^2/f_1^2)}{(1 - f^2/f_1^2) (1 - f^2/f_2^2) - 1} \quad (d)$$

To determine the resonance frequency f_r , the denominator is equated to zero; thus,

$$(1 - f_r^2/f_1^2) (1 - f_r^2/f_2^2) - 1 = 0$$

and solving for f_r :

$$f_r^2 = f_1^2 + f_2^2 \quad (e)$$

Substituting the specific values of M_1 , M and K given previously, it is found that resonant frequency $f_r = 67$ rad./sec. This value is used in the construction of the resonance response curves of Fig. 1.

The centrifugal force produced by the revolving eccentric is:

$$F_o = mrf^2 \quad (f)$$

where mr is the unbalance of the eccentric.

Substituting equation (f) into equations (c) and (d) and rearranging terms in order to put the equations in a dimensionless form, it is found that:

$$\frac{A_1}{mrf_r^2} = \frac{(f_1/f_r)^2 (f_2/f_r)^2}{(f/f_r)^2 - 1} \quad (g)$$

$$\frac{A}{mrf_r^2} = \frac{(f_1/f_r)^2 (f_2/f_r)^2 - (f/f_r)^2 (f_2/f_r)^2}{(f/f_r)^2 - 1}$$

Equations (g) and (h) are plotted in Fig. 1 with the left hand terms (called amplitude indexes) as a function of the ratio of the exciting to the resonant frequency (f/f_r). Both coordinates are therefore dimensionless.

At the operating frequency of 60 cps and with a test specimen in place, the frequency ratio (f/f_r) is approximately 0.114 and it may be noted from Fig. 1 that the amplitude of the cage and the frame are both negative. Hence both are in phase with each other but out of phase with the eccentric. Furthermore, the amplitude of the cage is significantly less than that of the frame. These results correspond with observations made during the calibration.

When the test specimen is replaced by the proving ring (having a significantly lower stiffness than the specimen) the resonant frequency f_r is considerably reduced. As a result, at the operating frequency of 60 cps the frequency ratio f/f_r increases to approximately 0.28 as shown in Fig. 1. For this case the cage is out of phase with the frame and in phase with the eccentric. Again, this theoretical conclusion was confirmed by observations during calibration of the machine.

2.5 Comparison of Results of the Three Methods of Calibration

The only method which measures the force F_s directly in the specimen is the SR-4 calibration. The SR-4 data are shown in Fig. 2 as the solid line and points (—●—). In this calibration the data were reproducible within approximately 25 lbs.

To determine the specimen force F_s by the other two methods it is of course necessary to consider the magnitude of inertia forces and their phase relationship to the centrifugal force, as discussed above and as diagrammed in Fig. 1. This is done below.

2.5.1 Theoretical Centrifugal Force Method. At the operating frequency with the test specimen in place the inertia force is 180° out of phase with the centrifugal force (see negative ordinate in Fig. 1 at frequency ratio indicated for case with test specimen in place). Thus:

$$F_s = F_e - F_i^s \quad (i)$$

where $F_s = \pm$ alternating force in the test specimen, lbs.

$F_e = \pm$ alternating force produced by the eccentric, $= mrf^2$, lbs.

$F_i^s = \pm$ inertia force caused by vibration of cage and associated parts with test specimen in place, lbs. $= M A_s f^2$

where A_s is amplitude of cage with specimen in place.

The values of F_e calculated directly from mrf^2 (where mr was both calculated and measured) are shown by the "O" points and dashed lines in Fig. 2. This F_e

curve must, of course, be "dropped" by the inertial force F_i^S , which was calculated by the equation (i) above. The resultant F_s curve is shown by the "O" points which fall along the solid line determined by SR-4 measurements within $\pm 1\frac{1}{2}\%$ in the operating range. Thus, the theoretical method checks the SR-4 method very closely.

2.5.2 Proving Ring Method. As discussed above, with the proving ring in the vibrating system (in place of the specimen) the cage motion is in phase with the eccentric (see positive ordinate in Fig. 1 for cage at operating frequency ratio with proving ring). Consequently, the alternating force F_p felt by the proving ring is:

$$F_p = F_e \pm F_i^p \quad (j)$$

where $F_i^p = \pm$ inertia force felt by vibrating cage and associated parts with proving ring in place, lbs.

$$= M A_p f^2$$

where A_p = amplitude of vibration of cage with proving ring in place.

Combining equations (i) and (j):

$$F_s = F_p - (F_i^p \pm F_i^S) \quad (k)$$

The values of F_p , determined directly from proving ring measurements are shown in Fig. 2 by the "O" points and dot-dash line. If this curve is dropped by the negative inertia force correction ($F_i^p \pm F_i^S$) as shown, the resultant F_s points, shown as "O", check the other two F_s curves within $\pm 1\frac{1}{2}\%$ in the operating range of the machine.

2.5.3 Conclusion. It is apparent from the data presented that all three methods of calibration check each other within $\pm 1\frac{1}{2}\%$ in the operating range, which is considered entirely adequate for fatigue testing.

III. Test Material

The N-155 material used in this investigation was furnished to the University of Michigan as part of an N.A.C.A. cooperative program (4).

Some of the specimens were prepared at Michigan, while others were prepared at Minnesota. In both cases a longitudinal polishing method (2) (4) was used to produce the final contour and surface finish. The chemical analysis, heat treatment and method of material processing and specimen preparation are described in reference 4.

IV. Test Specimens

The forms of the test specimens used are given in a previous report (2). All specimens have a 0.25" minimum diameter. At high alternating-to-mean stress ratios A (1.64 and higher), during which creep is not measured, a single fillet type "B" specimen is used; whereas at low stress ratios (0.67 and lower), where creep is measured, the type "A" specimen with a 2" effective gage length is used.

V. Test Procedure, Test Data, and Discussion

5.1 1000°F Tests

5.1.1 Temperature Production and Control Equipment. The furnace used and method of shunting for control of temperature uniformity was the same as used in previous work (1) (2). However, the temperature controller was quite different from these previously used. Since the temperature changes associated with damping energy (to be discussed later) are somewhat dependent on the type of controller used and the nature of the thermocouple mounting, these items are briefly discussed below.

The control system used temporarily until controls assigned to this work were received consisted of a Leeds and Northrup "Micromax" strip chart recorder controller, an associated control unit with adjustable proportional band and droop correction, and a motor-driven Variac. The variable voltage output of the Variac is connected to the furnace. Therefore, with this control system, whenever a change of specimen temperature occurs the control unit reacts to adjust the motor-driven Variac to increase or decrease its voltage output to the furnace. A similar control system is used with the controls assigned to this work. It consists of a Brown Elektronik circular chart recorder-controller with fixed (5%) proportional band and a motor-driven Powerstat. The control action is similar to the Leeds and Northrup equipment. With either of these control systems the temperature of the specimen is held to $\pm 5^\circ\text{F}$ of the thermocouple reading.

The temperature at the specimen is sensed by two chromel-alumel thermocouples wired to the minimum diameter of the specimen so as to maintain metallic contact and then covered with a platinum foil shield against radiation.

The thermocouple leads are then connected to a switching station outside the furnace which is so arranged to permit independent control and measurement of either thermocouple or both. During a normal test the thermocouples are connected in parallel to the controller thus giving an average emf to the controller and also enabling the temperature control to be maintained if one of the thermocouples fails during the test. Each of the thermocouples is checked with a portable potentiometer several times during a test.

In many of the tests at 1000°F the application of the alternating stress was accompanied by an immediate and large increase in specimen temperature. This temperature increase may be associated with damping capacity as explained later and is so rapid that even if the current to the furnace were reduced immediately to zero the specimen would still overheat in some cases. Consequently, it was necessary to devise auxiliary equipment in order to control this heating.

At first an air blast cooling device which admitted compressed air to the bottom of the furnace through a perforated copper tubing was added. This allowed a manually controlled volume of air to blow up through the furnace around the specimen thus decreasing any rate of temperature rise of the specimen too rapid to be controlled by the control system.

Later, two powerstats were connected in series with the eccentric motor starting circuit so that the otherwise constant speed (3600 RPM) motor could be closely controlled at various speeds in the range 3400-3600 RPM. By manually positioning the Powerstats the speed of the motor was regulated and consequently the applied alternating stress was controlled. By these means it was possible to control the heat generated by damping of the specimen to maintain the specimen at the desired temperature.

5.1.2 Test Procedure. The test specimen is assembled and properly aligned (2) in the high temperature grips and the thermocouples are attached. This assembly is then placed in the machine and properly attached to the top plate and eccentric cage with the usual precautions in order to minimize bending and prestressing (1). The thermocouple leads are connected to the switching station, the control system is activated and for the first six tests the following starting procedure was used. The specimen temperature was allowed to reach 800°F, purposely preset lower than test temperature to

compensate for any overheating due to damping energy. This initial heat-up period required 1/2 - 3/4 hour. At this temperature the alternating stress was applied to the specimen and at the same time the set point of the controller was raised to 980°F, allowing 20° for possible controller overshoot. The change in temperature of the specimen was noted by switching one of the thermocouples to the portable potentiometer. If a sudden rise in temperature due to damping in the specimen was noted at the start of the test the air blast was admitted to the furnace as described in the preceding section. After the specimen temperature ceased to rise the air blast was gradually reduced, allowing the electrical temperature controls to gradually take over before the test temperature of 1000°F was approached. After the specimen temperature had stabilized at 1000°F the controller was set at 1000°F and the test allowed to proceed without further adjustments except for periodic checks with the potentiometer to assure proper thermocouple and control readings.

It is realized that the interior of the test specimen may have been considerably hotter than the thermocouples which were more directly exposed to the air blast. However, by removing the air blast at a temperature as far below the test temperature as possible, by the time the specimen attained test temperature this temperature non-uniformity is minimized.

In most cases this air blast procedure effectively avoided overheating without additional precautions, but occasionally the heat caused by damping was so large and sudden as to require some changes in the procedure outlined above. This led to the development of the variable speed start-up equipment described previously and to the start-up procedure described next.

In the variable speed start-up procedure, the object is to maintain the temperature specimen as close to 1000°F as possible at all times. This is accomplished by controlling the speed of the eccentric motor so that any applied alternating stress is sufficient to maintain a steady state heat balance between damping energy in the specimen and external furnace heat. The stress is applied when the specimen temperature reached 1000°F, and is gradually applied by means of the variable speed arrangement until the temperature tends to rise abruptly. When this happens the applied stress is reduced by reducing the speed of the eccentric motor and the controller

then has time to reduce the input to the furnace. Both of these operations prevent drastic overheating of the specimen. This procedure is repeated until the specimen temperature remains constant at 1000°F and the eccentric motor is in synchronization at 3600 RPM. When this occurs the eccentric motor is switched over to line voltage and the variable speed start-up procedure is accomplished. While it was desirable to attain 3600 RPM as soon as possible, it required in most cases from 5 to 15 minutes of speeds in the 3200-3600 range. During the course of this start-up procedure the eccentric motor speed was determined by a tachometer and RPM readings taken at one minute intervals. The temperature of the specimen as recorded was checked with a Rubicon precision portable potentiometer.

In some tests slight overshooting (20°F) of specimen temperature occurred, but these are not believed to be serious. In other tests the specimen fractured before the full 3600 RPM speed necessary to apply predetermined alternating stress was attained. However, since the applied stress is proportional to the square of the frequency (or in this case, RPM) of the eccentric motor, the actual stress could be easily computed from the data taken on the speed of the motor. The "time to fracture" was computed on the basis of time at motor speed 3450 RPM and above. This permitted recording of rupture times on those specimens which fractured during the variable RPM start-up or shortly after full speed had been obtained. While this method of computing times is somewhat arbitrary and subject to errors, any error of time is believed to be less than 5%.

5.1.3 Test Results. The 1000°F test results are given in Table I and Figure 3. It is apparent from the footnotes that some of the tests may be invalid due primarily to the temperature increase caused by damping. This is particularly true of the tests conducted before the advent of the air blast and variable RPM starting procedure. Due to the overheating, some failure times are, no doubt, too short. Also, as indicated in the footnotes, some trouble was experienced due to furnace failure caused by the vibrations present in the test machine operating at the high stress levels used in the 1000°F tests.

A study is now being made of methods to utilize the nearly instantaneous temperature which occurs after the alternating force is applied to qualitatively determine the damping capacity of the material. One basic difficulty is, of course, that the damping observed is that associated with the material over a temperature range. However, it is felt that temperature increase observations can provide valuable information, which if considered with the damping data procured in rotating beam equipment (5) under carefully controlled conditions, would provide a more complete picture on the damping properties.

The temperature increase during start of test, as given in the footnotes in Table I, is of course only a rough qualitative indication of damping, particularly if air blast cooling is used. More significant are the temperature-time curves procured during the start of each test. The analysis of these temperature-time curves is now in progress with the objective of developing a starting procedure which might permit a more accurate indication of damping. Inspection of the slope of these temperature-time curves now available indicate that this damping appears to reach a peak value in the temperature range from 900-950°F, but this must be considered a tentative observation.

In the tests run to date, serious temperature increases did not occur at alternating stress below $\pm 40,000$ psi. It appears, therefore, that the damping-stress curve increases abruptly at this stress level.

5.2 Properties at Room Temperature

The fatigue properties of N-155 were determined at room temperature at two stress ratios, $A = 2.0$ and infinity, as shown in Table I and Fig. 3.

In only one case, specimen J-19 at the highest test stress (52,900 psi) was serious heating observed. For this specimen the damping caused the center 1/2" of the test section to attain a temperature of approximately 1500°F in less than 1 minute after the start of the test. Surprisingly, specimen JT-22 tested at the same stress (after a previous stress history - see test data, Table I) attained a temperature of approximately 400°F in about 20 minutes after the start of the test as measured by a thermocouple soldered onto the test section. Damping data for N-155 at room temperature to be presented in a future paper show that sustained cycle stress at room temperature decreases slightly the damping in the stress range cited above, and this would tend to cause the temperature increase of a specimen with a previous stress history to be reduced. However, the magnitude of this decrease does not appear to be sufficient to explain the different temperature observed in specimens J-19 and JT-22, and this discrepancy is being further investigated.

VI. SUMMARY AND CONCLUSIONS

The exciting and inertia force in the dynamic testing machine used in this work were carefully analyzed and calibrated. Three independent methods of calibration were used; one was essentially theoretical in nature and the other two were essentially experimental. All three methods of calibration checked each other within approximately $\pm 1\frac{1}{2}\%$ in the operating range.

The approximate reversed fatigue strength* at 1000°F indicated in Fig. 3 is $\pm 45,000$ psi. This strength must be considered only a tentative value because of the temperature increase difficulties experienced due to the high damping of N-155 as explained previously. Thus, the correct value is probably somewhat higher. There are no comparative direct stress data available. However, reversed bending fatigue strengths at 1000°F have been reported as (a) $\pm 49,000$ psi, about 10% higher than the direct stress value indicated above, on the identical material (4) and (b) $\pm 45,000$ psi on another heat of low carbon N-155 (6). The fatigue strength for a stress ratio of $A = 2.0$ at 1000°F is 19,700 psi \pm 39,300 psi. There is no other available data for comparative purposes.

The room temperature fatigue strength indicated in Fig. 3 is 21,200 \pm 42,400 psi at $A = 2$ and $\pm 46,500$ at $A = \infty$. Here again the only comparative data available for check purposes is the reversed bending fatigue strength of (a) $\pm 55,000$ psi (some 20% higher) on the identical material (4) and (b) $\pm 46,000$ psi** on another heat of material (6).

It is interesting to note that the reversed fatigue strength of N-155 at 1000°F is almost (within 5%) the same as the fatigue strength at room temperature whereas, at a stress ratio of $A = 2.0$, the fatigue strength at 1000°F is approximately 10% lower than at room temperature.

Most prior room temperature work indicated that in general the bending fatigue strengths of a material are significantly higher than the direct stress fatigue strengths. The fatigue data cited above are thus in agreement with this general observation. An analysis of the reasons for this difference between bending and direct stress fatigue strengths, although now in progress, is beyond the scope of this report.

*The term "fatigue strength" without further designation refers to the fatigue strength at 2×10^7 cycles.

**This is the fatigue strength of polished specimens. Ground and "rough" specimens had fatigue strengths of $\pm 38,000$ psi and $\pm 54,000$ psi, respectively, a difference which is probably attributable to surface stress (6).

The sudden increase in specimen temperatures observed immediately after the application of alternating force in certain temperature and stress ranges is an indication of the extremely high damping of N-155. Quantitative damping data on this material, discussed in Part C of report (7), partially confirm this observation.

This sudden temperature increase is caused by damping and introduces serious problems in testing techniques. An air blast cooling method incorporated within the specimen furnace, and lately a variable speed start-up procedure, has been reasonably successful in avoiding specimen overheating due to internal damping.

BIBLIOGRAPHY

1. B. J. Lazan, "Dynamic Creep and Rupture Properties of Temperature Resistant Materials Under Tensile Fatigue Stress", Air Force Technical Report No. 5930, February 1950.

Also see paper of same title in Proceedings, American Society for Testing Materials, Vol. 44, 1949, Pages 757 to 787.

2. Syracuse University, "Dynamic Creep, Rupture, Damping, and Elasticity Properties of Temperature Resistant Materials", Final Report on Air Force Contract W33-038 AC-15941, dated 14 February 1951.
3. Den Hartog, "Mechanical Vibrations" McGraw Hill, 1940.
4. N.A.C.A. Subcommittee on Heat-Resisting Materials "Cooperative Investigation of Relationship Between Static and Fatigue Properties of Heat-Resistant Alloys at Elevated Temperatures". N.A.C.A. No. 51A04, March 7, 1951.
5. B. J. Lazan and L. J. Demer, "Damping, Elasticity, and Fatigue Properties of Temperature-Resistant Materials", A.S.T.M. Proceedings, Vol. 51, 1951.
6. R. R. Ferguson, "Effect of Surface Finish on Fatigue Properties at Elevated Temperatures -I- Low Carbon N-155 with Grain Size of A.S.T.M.-1" N.A.C.A. Technical Report R M E 51D17, 26 June 1951.
7. Minnesota Annual Report titled "Dynamic Mechanical Properties of Temperature, Members, and Joints" on Air Force Contract AF-33 (038) - 18903, 1 March 1952.

TABLE I. TEST DATA FOR N-155

A:- ROOM TEMPERATURE TEST						
Spec. NO.*	Alter Mean Ratio A	Applied Stress - KSI				Time for Rupture in Hours
		Mean Stress	Alter Stress	Max. Stress	Min. Stress	
JU-23	2.0	21.0	41.2	62.2	-20.2	24.6 ^{1**}
JB-23	2.0	21.5	42.2	63.7	-20.7	152.
JE-21	2.0	22.1	43.2	65.3	-21.1	1.5 ^{2**}
JF-20	2.0	22.0	43.4	65.4	-21.4	18.2
JT-22 (1)	∞	0	44.2	44.2	-44.2	502. ³
JW-21	∞	0	47.0	47.0	-47.0	32.5
JT-22 (2)	∞	0	47.2	47.2	-47.2	267. ⁵⁴
JP-19	∞	0	52.9	52.9	-52.9	0.08 ⁵
JT-22 (3)	∞	0	52.9	52.9	±52.9	0.35 ⁶
B:- 1000°F TEST TEMPERATURE						
N1231F (1)	2.0	19.3	38.7	58.0	-19.4	117. ⁷
N1230F	1.8	21.0	37.9	58.9	-16.9	0.018 ⁸
JL19	2.0	19.7	39.3	59.0	-19.6	3.0
N1233F	2.0	19.7	39.3	59.0	-19.6	0.17 ⁹
N1234F	2.0	19.7	39.3	59.0	-19.6	48.1
N1231F (2)	2.0	20.0	40.0	60.0	-20.0	5.1 ¹⁰
N1232F	2.0	20.0	40.0	60.0	-20.0	4.4
JC20 (1)	∞	0	39.0	39.0	-39.0	271. ¹¹
JJ18 (1)	∞	0	41.0	41.0	-41.0	187. ¹²
JL22	∞	0	41.0	41.0	-41.0	0.13 ¹³
JS21	∞	0	43.4	43.4	-43.4	0.008 ¹⁴
JC20 (2)	∞	0	43.4	43.4	-43.4	0.025 ¹⁵
JJ18 (2)	∞	0	43.5	43.5	-43.5	0.13 ¹⁶
N1226F	∞	0	43.5	43.5	-43.5	0.05 ¹⁷
N1227F (1)	∞	0	43.5	43.5	-43.5	142. ¹⁸
N1228F	∞	0	45.0	45.0	-45.0	0.13 ¹⁹
N1227F (2)	∞	0	46.0	46.0	-46.0	168. ²⁰
N1235F	∞	0	46.5	46.5	-46.5	0.15 ²¹
N1227F (3)	∞	0	48.5	48.5	-48.5	0.65 ²²

*Specimen numbers with "J" prefix prepared by Michigan.

Specimen numbers with "N" prefix prepared by Minnesota.

**These elevated numbers indicate notes on following page.

TABLE I. TEST DATA FOR N-155 (CONTINUED)

Notes

1. Flex-plate (machine part) failed which bent specimen and stopped test.
2. Specimen fractured in the threads.
3. Test stopped before specimen ruptured.
4. Previous stress history. See JT-22 (1).
5. Test section of specimen attained dull red heat color with consequent elongation of specimen which stopped test.
6. Previous stress history. See JT-22 (1) and (2). Specimen temperature rose from 75° to approximately 400°F during duration of test.
7. Test stopped before specimen ruptured. Variable RPM start-up procedure used to control damping heat.
8. Specimen ruptured before machine attained 3600 RPM. Stress calculated on basis of maximum RPM attained. Variable RPM start-up procedure used to control damping heat.
9. Specimen temperature rose 20°F from 1000°F within 20 seconds after machine attained 3600 RPM. Variable RPM start-up procedure used to control damping heat.
10. Previous stress history. See N1231F (1).
11. Test stopped before specimen ruptured.
12. Test stopped before specimen ruptured. Air blast used to control specimen heating at approximately 825°F.
13. Specimen ruptured before machine attained 3600 RPM. Stress calculated on basis of maximum RPM attained. Variable RPM start-up procedure used to control damping heat.
14. Specimen temperature rose from 800° to approximately 1130°F within 30 seconds after machine attained 3600 RPM.
15. Previous stress history. See JC20 (1). Specimen temperature rose from 900° to approximately 1126°F within 90 seconds after machine attained 3600 RPM.
16. Previous stress history. See JJ18 (1). Specimen temperature rose from 900° to approximately 1150°F after machine attained 3600 RPM. Thermocouple failure occurred 2 minutes after starting test. Air blast used.
17. Specimen temperature rose from 950° to approximately 1040°F in about 20 seconds. Air blast used.
18. Variable RPM start-up procedure used to control damping heat.
19. Specimen temperature rose from 1000° to 1100°F. in approximately 30 seconds. Variable RPM start-up procedure used, specimen ruptured before machine attained 3600 RPM. Stress calculated on basis of maximum RPM attained.
20. Previous stress history. See N1227F (1). Variable RPM start-up procedure used to control specimen damping heat.
21. Specimen temperature rose from 1000° to 1030°F. at time of rupture. Variable RPM start-up procedure used.
22. Previous stress history. See N1227F (1) and (2) Specimen temperature rose from 1000 to 1030° F at time of rupture. Variable RPM start-up procedure used.

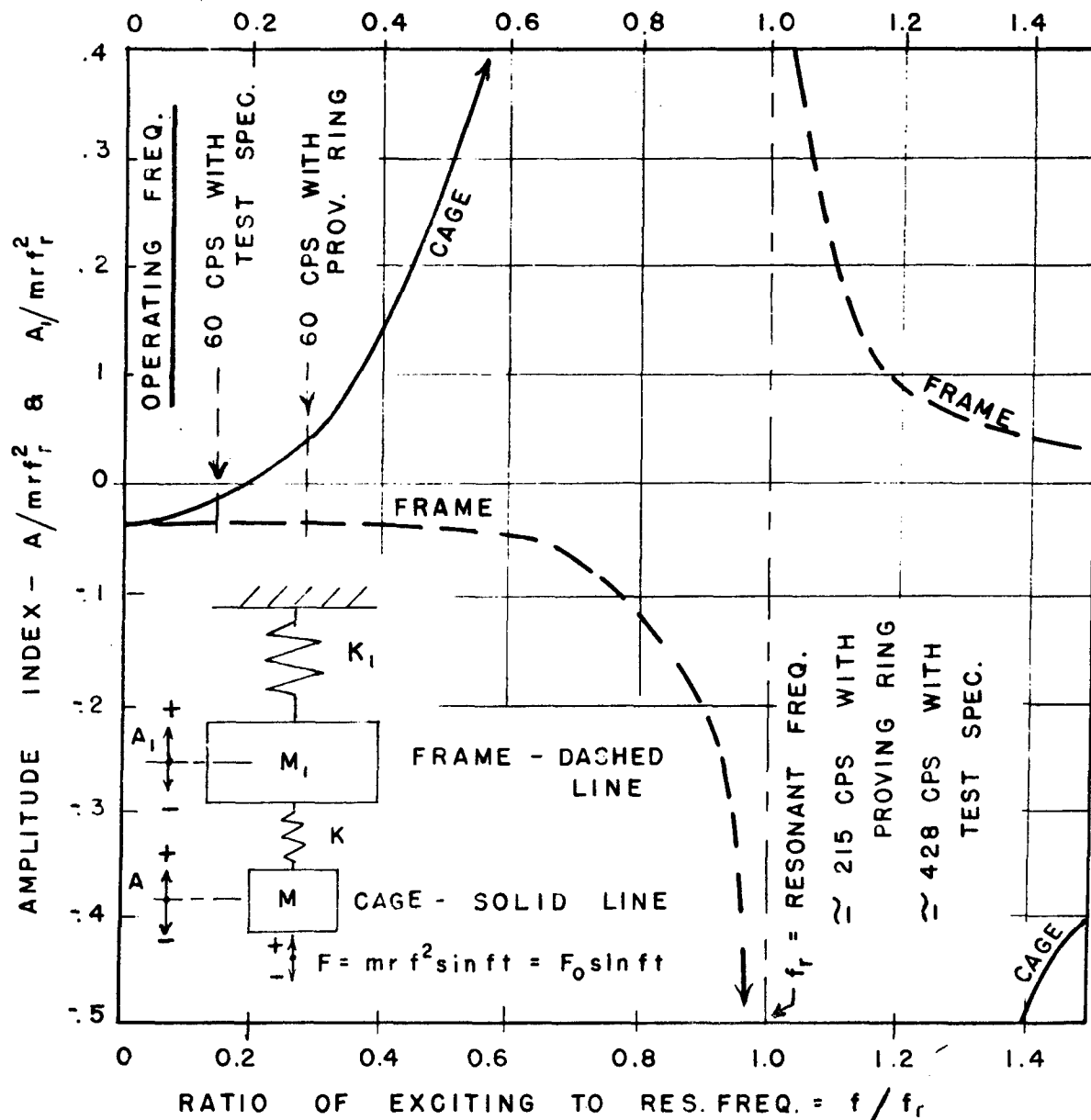


FIG. 1. AMPLITUDE FREQUENCY CURVES FOR MINNESOTA DIRECT STRESS FATIGUE MACHINES SHOWING LOCATION OF OPERATION FREQUENCIES

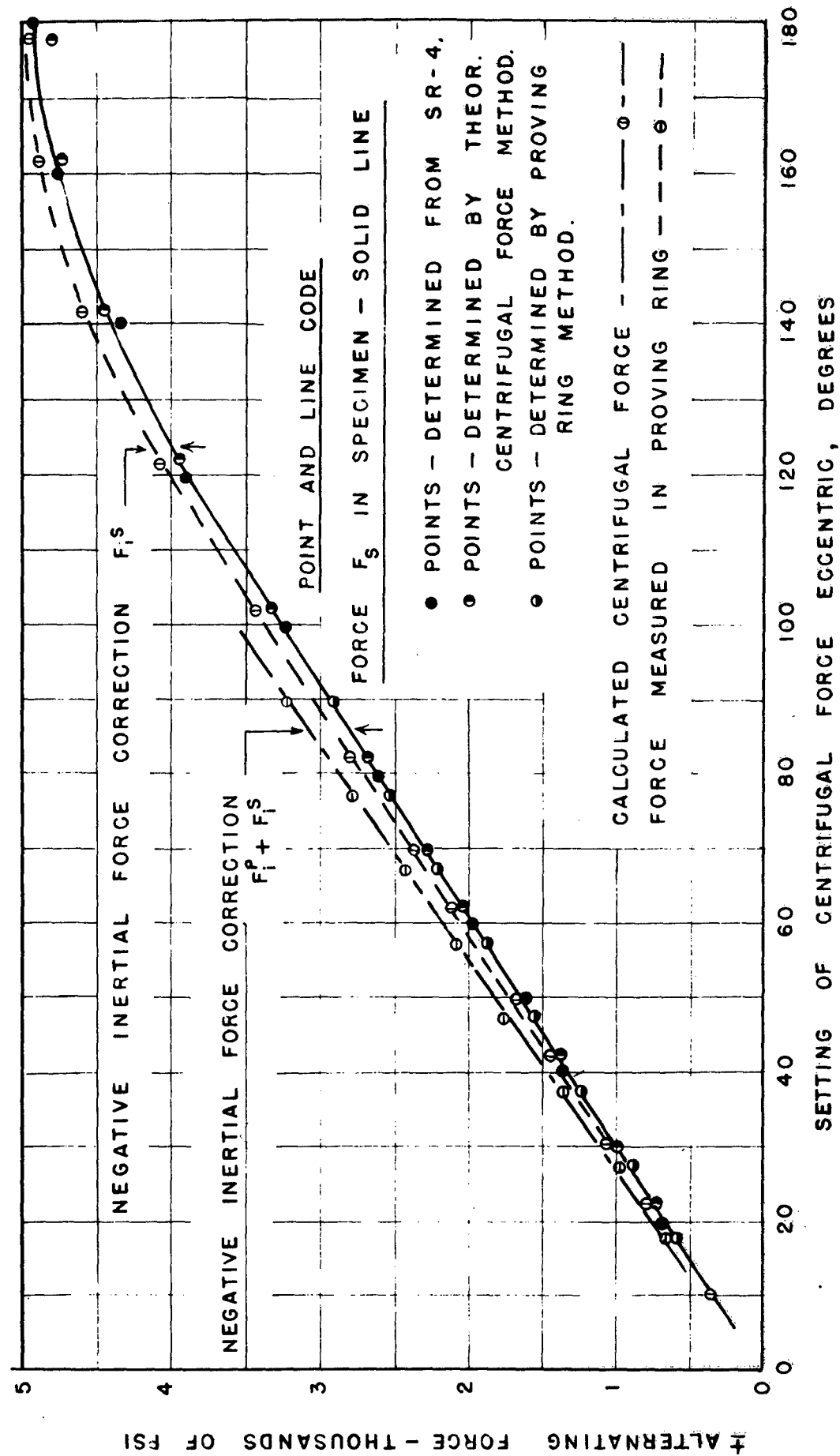


FIG.2. CALIBRATION CURVES FOR FATIGUE MACHINE NO. 6, SHOWING CHECK PROVIDED BY THREE INDEPENDENT METHODS.

